Imaging of steep flanks by focal sources

Jan Thorbecke
Delft University of Technology, The Netherlands

Abstract

One-way recursive wavefield extrapolation and migration has many advantages over other wavefield extrapolation methods. The method can handle complex models and is robust. However, the extrapolation of turning waves is one important omission of one-way wavefield extrapolation In this paper a new hybrid approach for the imaging of steep salt flanks is presented: CFP redatuming is used to redatum the data to a vertical array, and one-way wavefield extrapolation, using a rotated velocity field, is used to image the steep flank. A simple example is given for a synthetic data-set calculated for a model which includes a steep flank.

Introduction

Virtual sources can be simulated in the subsurface using a source array at the surface (Berkhout 1992, Rietveld et al. 1992). These virtual sources can be focussed (combined) again to illuminate specific parts of the subsurface. In the last section of Chapter 5 of Thorbecke (1997) an idea to image steep flanks was illustrated and briefly discussed, but has never been worked out. The last year this idea has been worked out in a slightly different way.

In short the idea boils down to the fact that an (vertical) array of focal points (FP's), with corresponding CFP-gathers and CFP-operators, is used to redatum surface data to the array of focal points. In Figure 1 two kinds of focal point arrays are shown; a vertical and a curved array. The response of this array is used to illuminate steeps flanks. The CFP redatuming, followed by imaging is worked out in this abstract and illustrated by imaging of a steep flank of a synthetic data set.

To redatum a data set, recorded at the surface, to a vertical array, focusing operators are needed which contain the propagation effects between the vertical array and the acquisition positions at the surface. A first focusing step creates CFP gathers which have virtual source positions on the vertical array and real detectors on the surface. After this first step a second focusing step is used, using the same focusing operators, but now with CFP gathers as input. After this second focusing step the focal point acts as a source position (where the focussing operator is confocal ($n = m$) with the focal point) and the other points in the vertical array, are receiver locations (where the focusing operators are bifocal ($n \neq m$) with the focal point). The CFP gather and the redatumed CFP gather are represented by

$$\mathbf{P}_j(z_0, z_n) = \mathbf{P}(z_0, z_0)\mathbf{F}_j(z_0, z_n), \quad (1)$$
$$\mathbf{P}_j(z_m, z_n) = \mathbf{F}(z_m, z_0)\mathbf{P}_j(z_0, z_n) \quad (2)$$

respectively. The constructed gathers $\mathbf{P}_j(z_n, z_m)$ can be migrated using a standard one-way shot record migration program, where the velocity model is rotated to become aligned with the new positions of the vertical array.

Zhang and McMechan (1997) used a similar approach, and also used a rotated velocity model of 90° to extrapolate the energy associated with turning waves, but they did not use a (CFP) redatuming step as introduced in this abstract. The redatuming step has two advantages:

- a smaller aperture is needed to migrate the reflection energy from the steep flank,
- the energy after redatuming is better focussed, which makes the (least squares) imaging condition better defined and more stable.
- after redatuming a detailed velocity analysis can be carried out to gain more insight in the velocities around the salt flank.

Example: salt flank model

To illustrate the CFP approach a synthetic steep flank model, shown in Figure 2a, is used. In this model 534 shots were modeled (using an acoustic finite-difference program) with a fixed-spread acquisition, ranging from 0 to 8000 m, and a source and receiver spacing of 15 m. The model consists of a background model with a vertical velocity gradient and a salt-like structure on the right hand-side of the model. The recorded wavefield from shots on the left hand-side of the model, will contain energy from reflected turning waves. The dotted line in Figure 2a indicates the vertical positions of the focal points (FP's), each FP being connected to a CFP-gather. The vertical distance between the FP positions in the vertical array is chosen ($\Delta z = 15$ m.). These vertical FP positions will become the 'new' acquisition plane. The snapshots in Figure 2a show that the reflection of the steep flank contains multiple arrivals. Figure 2b shows a shot record with a source position in the outer left part of the model ($x = 105$ m). The reflection from the top of the salt and multiple arrivals from the steep flank are clearly visible.

Two pre-stack depth migration results, using the modelled shots, are shown in Figure 3. The true model as used in the FD modelling, was also used in the one-way migration. For the Kirchhoff migration a smoothed model was used for the modelling of the rays. The Kirchhoff migration (Figure 3a) images the steep flank close to 90° degrees and the one-way based scheme (Figure 3b) close to 70°. In these results one can see that the overturned part in the middle of the flank (around $z = 2000$ m) is not imaged by these migration methods. In the one-way result (b) the bottom of the salt and the bottom of the overhang of the salt, are imaged by reflection energy which has travelled through the salt body.

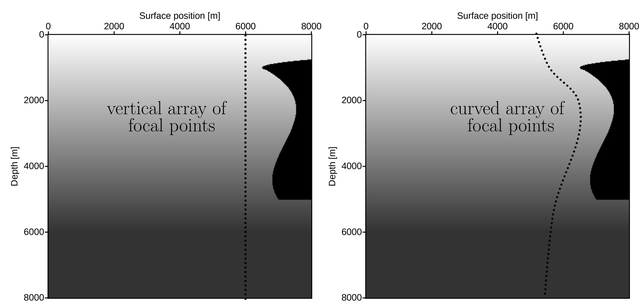

FIGURE 1: *An array of focal points can be used as a redatuming surface. This array can be designed to illuminate the structure in an optimum way. In this abstract we use a vertical array of focal points as shown in the left picture.*

The focusing operators, used to construct the CFP gathers at the vertical array of Figure 2a, are calculated using a ray-based modeling program. These calculated focussing operators will correctly follow the turning waves through the model. The velocity model used for the ray-based modelling only contains the background model: a depth velocity gradient of 0.4 m/s per meter ranging from 0 to 6000 meter and starting at $z = 0$ with 1500 m/s. Usually the velocity gradient along the side(s) of a salt structure is well known. On positions of the vertical array, where the focal point coincides with a reflecting boundary, the calculated operator can be verified using the CFP principle of equal traveltime. If one has measurements from buried detectors, then the first arriving event in these measurements (Xiao et al.,2006) can also be used to constrain and verify the calculated focussing operators.

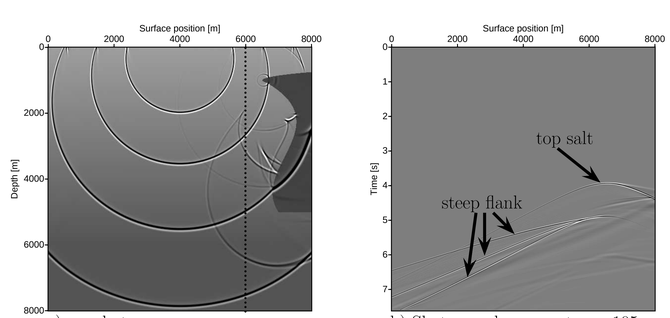

a) snaphots b) Shot record source at $x = 105, z = 0$.

FIGURE 2: *Salt dome model embedded in a medium with a vertical velocity gradient. The vertical array at x=6000 shows the 533 locations ($\Delta z = 15$) of the FP's, each FP being connected to a CFP-gather. Note the complex, multi-valued, wavefront from the reflection of the steep salt flank in the snapshots (a). Multiple arrivals in the turning wave event occur around 6 s. in the shot record from the far left side of the model (b).*

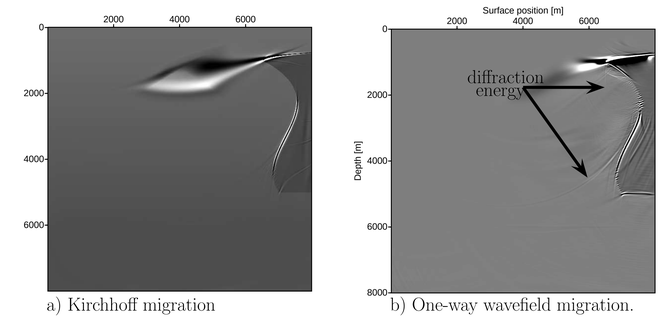

a) Kirchhoff migration b) One-way wavefield migration.

FIGURE 3: *Pre-stack depth migration results using original shots records (not redatumed) with Kirchhoff migration (a) and recursive one-way wavefield migration (b). In the one-way results parts of the steep flank are imaged due to the presence of diffraction energy originating from course blocks in the finite difference model.*

The constructed CFP gather in Figure 4a, includes reflection energy from the steep flank which has propagated through the vertical gradient medium. The reflection event in the CFP gather around 4 s. originates from the steep flank of the salt. After constructing all CFP gathers at the defined vertical array, the redatuming step is completed by using the focusing operators a second time. Applying this redatuming step to all CFP gathers gives a new pre-stack volume. For one redatumed source position the constructed shot record is shown in Figure 4b. This redatumed CFP gather can be interpreted as the response of a source at $x = 6000, z = 1500$ with receivers at the vertical line $x = 6000, z = [15 - 7995]$. In this redatumed shot record multi-valued arrivals from the synclinal structure of the flank are visible and indicated with an arrow. The application of this redatuming process gives 533 shot records, each with 533 receivers and one virtual source positioned on the defined vertical array.

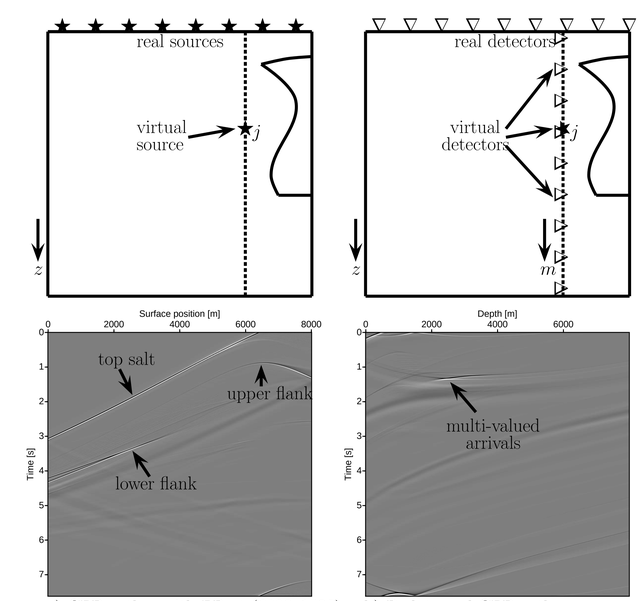

a) CFP gather with FP at $(6000, 1500)$ b) Redatumed CFP gather

FIGURE 4: *CFP gather for focal points at depth of 1500 m after the first (a) focussing step and after redatuming to the vertical array at $x = 6000$ (b). Note that the horizontal axis in a) represents surface position of the real sources, and in b) the horizontal axis represents depth positions of virtual positions on the array.*

Imaging of steep flanks by focal sources

Jan Thorbecke
Delft University of Technology, The Netherlands

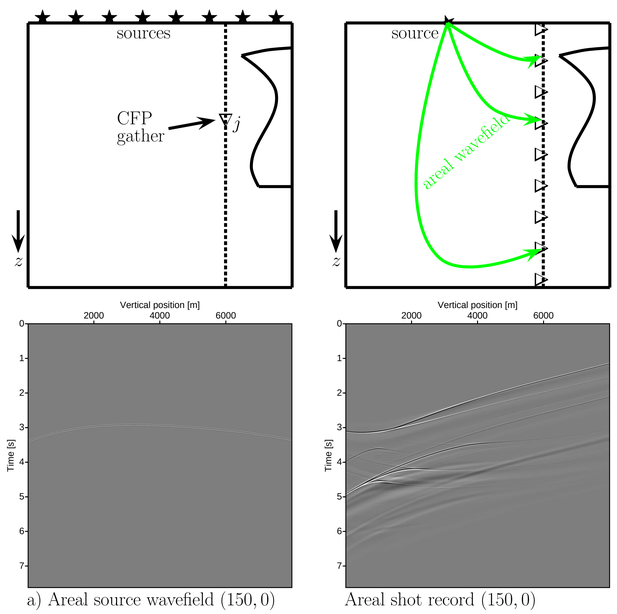

a) Areal source wavefield $(150, 0)$ Areal shot record $(150, 0)$

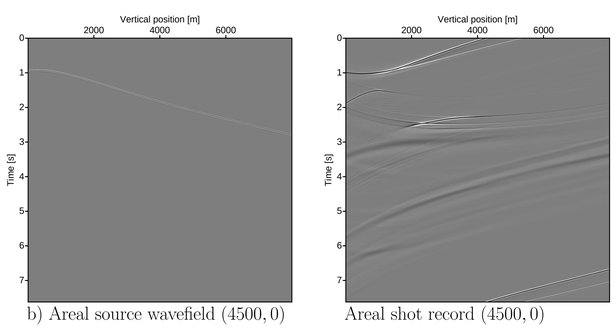

b) Areal source wavefield $(4500, 0)$ Areal shot record $(4500, 0)$

FIGURE 5: *Using the CFP gathers and their operators one can resort their traces to construct areal wavefields which show the contribution of one shot to the redatumed array (green lines in the top figure). Two contribution are calculated one for a shot at $x = 150$ (a) and one at $x = 4500$ (b).*

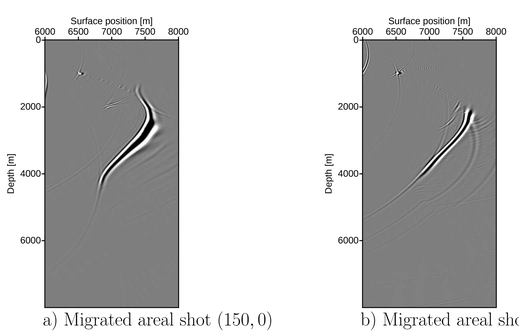

a) Migrated areal shot $(150, 0)$ b) Migrated areal shot $(4500, 0)$

FIGURE 6: *Areal shot record migration of the Figure 5a (a) and Figure 5b (b). The migration result of the shot at $x = 150$ clearly show the contribution of overturned energy. The shot with source at $x = 4500$ contains almost no energy of the steep flank.*

By adding the sources within a redatumed common receivers gather together, a plane wave response is constructed and shown in Figure 7a. This response is migrated through a rotated velocity model shown in the background of Figure 7c. The plane-wave migration result in Figure 7c shows that indeed energy from the steep flank has been preserved and can be imaged with one-way operators using a 90° rotated velocity model. This simple plane wave test already indicates that turning wave energy has been preserved in the CFP redatuming.

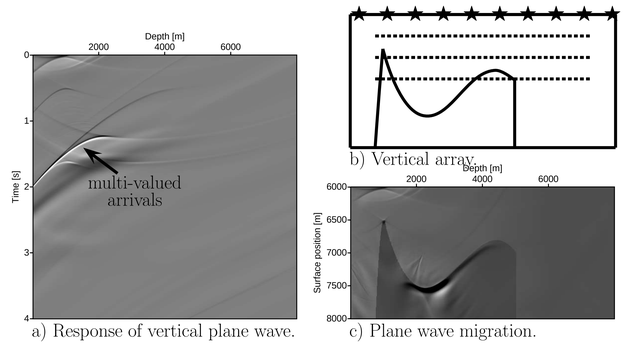

a) Response of vertical plane wave. b) Vertical array. c) Plane wave migration.

FIGURE 7: *Response of vertical plane wave (a) by the vertical array (b). This plane wave response is migrated using a rotated velocity model. The result of the plane wave migration is shown in c).*

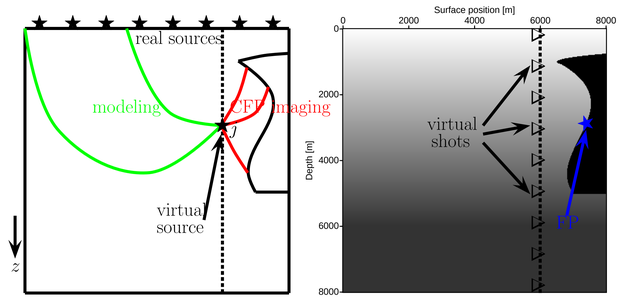

FIGURE 8: *For the imaging of steep flanks a two step procedure is proposed. In the first step focusing operators (one-way Green's functions) are modeled in a background model and surface data is redatumed to a vertical array of focal points. The second step standard (CFP) migration analysis is used to image the steep reflector. To check the velocity model, used to migrate the redatumed data, CFP analysis can be used for focal points (blue star) on the flank.*

To verify the velocity model (or focussing operators) of the salt flank structure the redatumed data set can also be used to construct CFP gathers with FP's on the flank, and check 'the principle of equal traveltime'. Indicated in Figure 8 a focal point (blue star) on the flank of the salt dome is chosen at $z = 3000, x = 7330$, a focusing operator is calculated, and CFP gather constructed. Figure 9a shows the CFP gather with its focussing operator overlaid. Note that the operator verification, using the reflections from the steep flank, can lead to accurate focusing operators.

Migrating the redatumed CFP gathers with a pre-stack depth migration algorithm gives the image shown in Figure 9c. For comparison in Figure 9b the same area for the pre-stack depth migration result (Figure 3b) is shown for surface shot record migration. The same one-way wavefield extrapolation operators are used (Thorbecke et al., 2004). Note the better imaging of the steep flank of the salt structure. The reflection of the flank is too steep to be imaged with one-way operators and recorded data at the surface. One-way extrapolation operators, applied on recorded data at the surface and using a regular grid, cannot handle turning waves, so the energy of the turning waves, which are visible in Figure 2b, is suppressed by the one-way operators, and not imaged in Figure 9b. Note that reflections of the top and bottom of the salt, which has travelled through the salt, are nicely imaged. Note also that parts of the steep flank are imaged due to the presence of diffraction energy originating from course blocks in the finite difference model. This imaged diffraction energy is visible as horizontally oriented events which are not aligned with the steep flank.

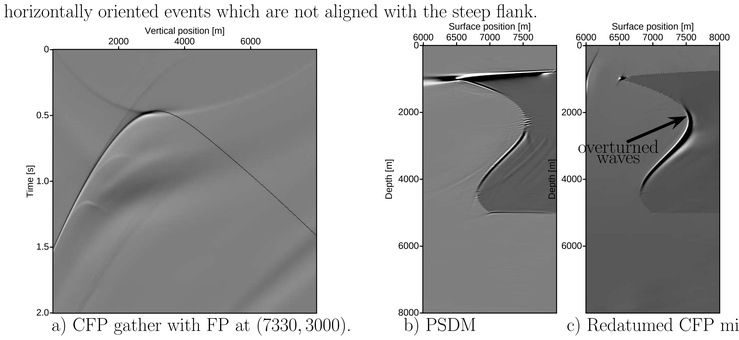

a) CFP gather with FP at $(7330, 3000)$. b) PSDM c) Redatumed CFP migration

FIGURE 9: *Focusing analysis on the rotated flank of the salt structure can be used to check the correctness of the focusing operators (a). The operator (shown as the black line superimposed on the CFP gather) and the CFP gather have the same traveltime indicating that the correct operator was used.*
Comparison between conventional shot record (b) and redatumed CFP gather (c) migration. Note that the CFP gather images the flank much better and also images the turning waves (indicated with an arrow). Due to the diffractors at the grid corners (staircase effect) of the coarse grid in the finite difference model, the steep flank in (b) is partly imaged due to the presence of diffraction energy. This diffraction energy is also clearly present at the base of the structure.

Conclusions

Redatumed CFP gathers can be used to image complex geological structures which contain steep flanks. The proposed procedure consists of three steps: First a slant or vertical or curved array of focal points with their CFP gathers is constructed. Second the CFP gathers are redatumed to the array positions. The redatumed CFP gathers represent a fixed acquisition spread along the array of focal points. Thirdly, these redatumed CFP gathers are input to standard velocity analysis and then migrated by a standard shot record migration program. Note that the position of the structure can be verified by using the principle of equal travel time. The obtained migrated image will show information of high angles and overturned waves when these are present in the data. For an optimal imaging and detailed velocity analysis the virtual array can be designed for any specific geological structure.

Acknowledgements

The author would like to thank the sponsors of the DELPHI consortium for their financial support.

References

Berkhout, A. J., 1992, Areal shot record technology: Journal of Seismic Exploration, **1**, 251–264.
Krebs, J. R., D. R. Fara, and A. E. Berlin, 1996, Accurate migration using offset-checkshot surveys: 58th Ann. Internat. Mtg., Expanded Abstracts, Session:X020, Eur. Assoc. Expl. Geophys.
Rietveld, W. E. A., A. J. Berkhout, and C. P. A. Wapenaar, 1992, Optimum seismic illumination of hydrocarbon reservoirs: Geophysics, **57**, 1334–1345.
Thorbecke, J., K. Wapenaar, and G. Swinnen, 2004, Design of one-way wavefield extrapolation operators, using smooth functions in WLSQ optimization: Geophysics, **69**, 1037–1045.
Thorbecke, J. W., 1997, Common focus point technology: PhD thesis, Delft University of Technology.
Xiao, X., M. Zhou, and G. T. Schuster, 2006, Salt-flank delineation by interferometric imaging of transmitted P- to S-waves: Geophysics, **71**, SI197–SI207.
Zhang, J. and G. A. McMechan, 1997, Turning wave migration by horizontal extrapolation: Geophysics, **62**, 291–297.